Semiconducting Tin and Lead Iodide Perovskites with Organic Cations: Phase Transitions, High Mobilities and Near-infrared Photoluminescent Properties

Constantinos C. Stoumpos, Christos D. Malliakas and Mercouri G. Kanatzidis

Department of Chemistry, Northwestern University, Evanston, Illinois 60208, U.S.A.

Supporting Information

Synthesis

Sn granules, I_2 (99.8%), $HC(NH_2)_2Cl$ (98%), $Pb(NO_3)_2$ (99.999%), KI (99.0%) and CsI (99.95%) solids and distilled HI 57% (99.95%), H_3PO_2 50% and CH_3NH_2 40% aqueous solutions and MeONa 25% methanolic solution were purchased by Sigma-Aldrich.

SnI_2 was prepared by a modification of the literature method:[1]

A 3-necked 500 mL bottom round flask is charged with 50g granulated Sn and 300 mL of 2M aqueous HCl is added. The mixture is flushed with N_2 for 1-2 min. 70g of I_2 are added in two portions. The solution turns to dark brown. The flask is immersed in a silicon oil bath heated to 170 ˚C and attached to a condenser. At this point the N_2 flow should be minimum, in order to avoid I_2 fumes to escape or crystallize inside the condenser. When the atmosphere inside the flask is free of I_2 vapors, 50 mL of 2M HCl is added, to transfer the quantity of I_2 that has crystallized inside the condenser back into the flask. At this point, the N_2 flow is increased slightly. As the reaction proceeds the color of the solutions changes progressively to red and finally to yellow. When the color of the solution turns yellow (takes 60-120 minutes), Sn is added to the mixture at 15 min time intervals in ~1g batches. This is because it is necessary to remove any traces of I_2 or, less likely, O_2 present. The reaction is judged to be complete, when the color of the solution is *bright* yellow and the Sn added retains its luster for 15 minutes. The yellow solution is transferred by decantation (since Sn is granulated filtering is not required) to a 500 mL 2-necked flask, which is immersed on a water bath heated at 70 ˚C under a flow of N_2. The hot yellow solution is slowly brought to ambient temperature and the first crystals of SnI_2 crystallize as long red needles. This cooling step encourages the formation of larger crystals which facilitate the isolation of the material. The precipitation is complete on standing overnight. After 1 day, large red needles of SnI_2 have been formed. The product is isolated either by filtration, followed by copious washing with 0.01M degassed HCl and drying in a vacuum oven at 50^{o}C, or through evaporation to dryness at 70^{o}C. The yield is 90-100g (90-99% based on total I_2) of pure SnI_2. The dried solid has a bright red color and is stable on standing in dry air for several weeks. Combined action of oxygen and water on the material results in rapid oxidation to orange SnI_4, while distilled water causes hydrolysis to white $Sn(OH)_2$.

PbI_2 was prepared by mixing aqueous solutions of $Pb(NO_3)_2$ and KI in 1:2 molar ratio. CH_3NH_3I was prepared by neutralizing equimolar amounts of HI and aqueous CH_3NH_2. $HC(NH_2)_2I$ was prepared by neutralizing EtOH solutions of $HC(NH)(NH_2)$ (prepared by neutralizing $HC(NH_2)_2Cl$ with MeONa in MeOH

and discarding NaCl) with aqueous HI. The purity of the materials was confirmed by powder diffraction measurements. The experimental diffraction patterns versus the calculated ones are given in Figures S2-S4.

A) Solution synthesis

General procedure: A 100 ml 2-necked round bottom flask was charged with a mixture of aqueous HI (6.8 ml, 7.58M) and aqueous H_3PO_2 (1.7 ml, 9.14M). The liquid was degassed by passing a stream of nitrogen through it for 1 min and keeping it under a nitrogen atmosphere throughout the experiment. SnI_2 (372 mg, 1 mmol) or PbI_2 (462 mg, 1 mmol) was dissolved in the mixture upon heating the flask to 120^{o}C using an oil bath, under constant magnetic stirring, forming a *bright* yellow solution.

$CH_3NH_3SnI_3$ (1): A 100 ml 2-necked round bottom flask was charged with a mixture of aqueous HI (6.8 ml, 7.58M) and aqueous H_3PO_2 (1.7 ml, 9.14M). The liquid was degassed by passing a stream of nitrogen through it for 1 min and keeping it under a nitrogen atmosphere throughout the experiment. SnI_2 (372 mg, 1 mmol) was dissolved in the mixture upon heating the flask to 120^{o}C using an oil bath, under constant magnetic stirring, forming a *bright* yellow solution. To the hot yellow solution was added solid CH_3NH_3I (159 mg, 1 mmol) which dissolved immediately. The solution was evaporated to approximately half its original volume by heating at 120^{o}C. The stirring was discontinued and the solution was left to cool back to room temperature. Upon cooling, *black*, elongated, rhombic dodecahedral (12 faces) crystals of the title compound were precipitated. The crystals were left to grow inside the mother liquor for a further 24 h under a nitrogen atmosphere before being filtered and washed copiously with *degassed* EtOH. Yield 70-90%. (*D*iffuse-*R*eflectance *I*nfrared *F*ourier *T*ransformed spectroscopy, DRIFT)KBr: 3393br, 3191br, 2961w, 2925w, 2855w, 1623s, 1471m, 1383w, 1320w, 1260m, 1124s, 1061s, 806w, 566w. On exposure to the atmosphere, the lustrous black crystals develop some irredesence on their surface in the first few minutes of exposure before gradually converting into black/greenish dull solid after approximately 24h.

$HC(NH_2)_2SnI_3$ (2): A 100 ml 2-necked round bottom flask was charged with a mixture of aqueous HI (6.8 ml, 7.58M) and aqueous H_3PO_2 (1.7 ml, 9.14M). The liquid was degassed by passing a stream of nitrogen through it for 1 min and keeping it under a nitrogen atmosphere throughout the experiment. SnI_2 (372 mg, 1 mmol) was dissolved in the mixture upon heating the flask to 120^{o}C using an oil bath, under constant magnetic stirring, forming a *bright* yellow solution. To the hot yellow solution was

added solid $HC(NH_2)_2I$ (172 mg, 1 mmol) dissolving immediately. The solution was evaporated to approximately half its original volume by heating at 120°C. The stirring was discontinued and the solution was left to cool back to room temperature. Upon cooling, *black* rhombic dodecahedral crystals (12 faces) of the title compound were precipitated. The crystals were left to grow inside the mother liquor for a further 24 h under a nitrogen atmosphere before being filtered and washed copiously with degassed EtOH. Yield 70-90%. DRIFT, KBr: 3402br, 3269br, 2926w, 2925w, 1714s, 1624w, 1400m, 1111m, 1065s, 810, 598w. On exposure to the atmosphere, the lustrous black crystals develop some irredesence on their surface in the first few minutes of exposure before gradually converting into black/greenish dull solid after approximately 24h.

$CH_3NH_3PbI_3$ (3): A 100 ml 2-necked round bottom flask was charged with a mixture of aqueous HI (6.8 ml, 7.58M) and aqueous H_3PO_2 (1.7 ml, 9.14M). The liquid was degassed by passing a stream of nitrogen through it for 1 min and keeping it under a nitrogen atmosphere throughout the experiment. PbI_2 (462 mg, 1 mmol) was dissolved in the mixture upon heating the flask to 120°C using an oil bath, under constant magnetic stirring, forming a *bright* yellow solution. To the hot yellow solution was added solid CH_3NH_3I (159 mg, 1 mmol) dissolving immediately. The solution was evaporated to approximately half its original volume by heating at 120°C. The stirring was discontinued and the solution was left to cool back to room temperature. Upon cooling, *black*, rhombic dodecahedral crystals (12 faces) of the title compound precipitated. The crystals were left to grow inside the mother liquor for a further 24 h under a nitrogen atmosphere before being filtered and washed copiously with *anhydrous* EtOH. Yield 70-90%. DRIFT, KBr: 3529br, 3180br, 2956w, 2925w, 2711w, 1599s, 1471m, 1250m, 1056m, 960m, 910m, 492m. The crystals are insensitive on exposure to the atmosphere but spontaneously hydrolyse to yellow PbI_2 upon wetting in H_2O. They retain their luster for several weeks after which time their surface becomes dull, without, however, affecting the integrity of the solid.

$HC(NH_2)_2PbI_3$ (4a): A 100 ml 2-necked round bottom flask was charged with a mixture of aqueous HI (6.8 ml, 7.58M) and aqueous H_3PO_2 (1.7 ml, 9.14M). The liquid was degassed by passing a stream of nitrogen through it for 1 min and keeping it under a nitrogen atmosphere throughout the experiment. PbI_2 (462 mg, 1 mmol) was dissolved in the mixture upon heating the flask to 120°C using an oil bath, under constant magnetic stirring, forming a *bright* yellow solution. To the hot solution was added solid $HC(NH_2)_2I$ (172 mg, 1 mmol) dissolving immediately. The solution was evaporated to approximately half its original volume by heating at 120°C. The stirring was discontinued and the

solution was left at 100°C to evaporate slowly. *Black* hexagonal (8 faces) or trigonal (5 faces) crystals of the title compound were precipitated and grown at this temperature. After standing for 2-3 h at 100 °C, under a nitrogen atmosphere, the temperature was set to 80 °C for a further 2-3 h. The step was repeated two more times to reach 60°C and 40°C at which point the solution was left to come to room temperature by powering off the hotplate. The crystals were collected by filtration and washed copiously with anhydrous EtOH. Yield 50-60%. DRIFT, KBr: 3345br, 2938s, 2858s, 1691s, 1656s, 1543m, 1139s, 1066s, 608m, 430w. Upon exposure to the atmosphere, at ambient temperature, the compound totally converts to **4b** within 1h. Hydrolyses in water to PbI_2.

$HC(NH_2)_2PbI_3$ (4b): A 100 ml 2-necked round bottom flask was charged with a mixture of aqueous HI (6.8 ml, 7.58M) and aqueous H_3PO_2 (1.7 ml, 9.14M). The liquid was degassed by passing a stream of nitrogen through it for 1 min and keeping it under a nitrogen atmosphere throughout the experiment. PbI_2 (462 mg, 1 mmol) was dissolved in the mixture upon heating the flask to 120°C using an oil bath, under constant magnetic stirring, forming a *bright* yellow solution. To the hot yellow solution was added solid $HC(NH_2)_2I$ (172 mg, 1 mmol) dissolving immediately. The solution was evaporated to approximately half its original volume by heating at 120°C. The stirring was discontinued and the solution was left at 100°C to evaporate slowly. Black hexagonal (8 faces) or trigonal (5 faces) crystals were precipitated. At that point, heating was discontinued and the mixture was cooled to room temperature. After 4-5 h the black crystals fully convert to *yellow* ones of essentially the same shape. The yellow crystals were collected by filtration and washed copiously with anhydrous EtOH. Yield 50-60%. The crystals are insensitive on exposure to the atmosphere but spontaneously hydrolyse to yellow PbI_2 upon wetting in H_2O. **$CH_3NH_3Sn_{1-x}Pb_xI_3$ solid solutions (5):** A 100 ml 2-necked round bottom flask was charged with a mixture of aqueous HI (6.8 ml, 7.58M) and aqueous H_3PO_2 (1.7 ml, 9.14M). Mixtures of SnI_2 (279 mg, 0.75 mmol, **5a**; 186 mg, 0.50 mmol, **5b**; and 93 mg, 0.25 mmol, **5c**), and PbI_2 (116 mg, 0.25 mmol, **5a**; 231 mg, 0.50 mmol, **5b**; and 347 mg, 0.75 mmol, **5c**) were dissolved forming a bright yellow solution which was heated to 120°C using an oil bath. To the hot solution was added solid CH_3NH_3I (159 mg, 1 mmol) dissolving immediately. The solution was evaporated to approximately half its original volume by heating at 120°C. The stirring was discontinued and the solution was left to cool back to room temperature. Upon cooling, *black*, rhombic dodecahedral crystals (12 faces) or truncated octahedral (14 faces), depending on the crystallization temperature or/and the composition, precipitated. The crystals were left to grow inside the mother liquor for a further 24 h under a nitrogen atmosphere before being filtered and washed copiously with *degassed* EtOH. The solid solutions reflect

the properties of their parent compounds. Sn-containg solids are air sensitive and Pb-containing ones are readily hydrolysable.

$CsSnI_3$ (6a): A 100 ml 2-necked round bottom flask was charged with a mixture of aqueous HI (6.8 ml, 7.58M) and aqueous H_3PO_2 (1.7 ml, 9.14M). The liquid was degassed by passing a stream of nitrogen through it for 1 min and keeping it under a nitrogen atmosphere throughout the experiment. PbI_2 (462 mg, 1 mmol) was dissolved in the mixture upon heating the flask to 120^{o}C using an oil bath, under constant magnetic stirring, forming a *bright* yellow solution. To the hot yellow solution was added solid CsI (260 mg, 1 mmol) dissolving immediately. 2 min after the addition of the *yellow* needle-shaped crystals started to precipitate. The stirring was discontinued and the solution was left to cool to room temperature. The crystals were left to grow inside the mother liquor for a further 24 h under a nitrogen atmosphere before being filtered and washed copiously with degassed EtOH. With this sample there is almost always a Cs_2SnI_6 (**9b**) impurity which forms spontaneously upon addition of solid CsI into the solution. Pure yellow needles can be obtained by adding a solution of CsI in 1 mL of concentrated HI over the course of 2 min. Yield 80-90%. The compound is air sensitive as demonstrated by the full conversion of the yellow crystals into a black solid within 24h. The black solid is **6b**.

Cs_2SnI_6 (6b): A 100 ml 2-necked round bottom flask was charged with a mixture of aqueous HI (6.8 ml, 7.58M) and aqueous H_3PO_2 (1.7 ml, 9.14M). The liquid was degassed by passing a stream of nitrogen through it for 1 min and keeping it under a nitrogen atmosphere throughout the experiment. SnI_2 (372 mg, 1 mmol) was dissolved in the mixture upon heating the flask to 120^{o}C using an oil bath, under constant magnetic stirring, forming a *bright* yellow solution. To the hot yellow solution was added solid CsI (260 mg, 1 mmol) dissolving immediately. 2 min after the addition of the yellow needle-shaped crystals started to precipitate. The precipitate was dissolved by adding 10 mL of acetone producing a dark red solution. After 5 min the stirring was discontinued and the solution was left to cool to room temperature. *Black* truncated octahedral (14 faces) crystals were formed upon standing. The crystals were left to grow inside the mother liquor for a further 24 h under a nitrogen atmosphere before being filtered and washed with degassed EtOH. Yield 80-90%. The compound is air- and water-stable. It forms black aqueous solutions which decompose only slowly to deposit white SnO_2 and deep red I_3^- solutions.

$CsPbI_3$ (7): A 100 ml 2-necked round bottom flask flask was charged with a mixture of aqueous HI (6.8 ml, 7.58M) and aqueous H_3PO_2 (1.7 ml, 9.14M). The liquid was degassed by passing a stream of nitrogen through it for 1 min and keeping it under a nitrogen atmosphere throughout the experiment. PbI_2 (462 mg, 1 mmol) was dissolved in the mixture upon heating the flask to 120^{o}C using an oil bath,

under constant magnetic stirring, forming a *bright* yellow solution. To the hot yellow solution was added solid CsI (260 mg, 1 mmol) immediately producing a *yellow* precipitate. The precipitate was redissolved by adding the minimum required amount of acetone ~5 mL. Stirring was discontinued and the solution was left to cool to room temperature. Yellow needle-shaped crystals were formed upon standing. The crystals were left to grow inside the mother liquor for a further 24 h under a nitrogen atmosphere before being filtered and washed copiously with anhydrous EtOH. Yield 80-90%. The compound is insensitive to air but it hydrolyses spontaneously.

B) Solid state reactions

1) *Sealed tube preparations*: Equimolar amounts of MI_2 and AI were loaded in a 9mm pyrex tube. Typically, the scale is 1 mmol based on the Sn or Pb halide. The materials were shaken mechanically to ensure a homogenous mixture. The tube was placed on a sealing line, evacuated to 10^{-4} mbar, and flame sealed. The tube was immersed on a sand bath standing a 200^{o}C, in such a way that the mixture of solids was heated homogeneously. About 4/5 of the tube was maintained outside the bath at room temperature. The solids were left in the bath for 2 h forming a homogeneous black solid. The Sn-containing solids are air sensitive whereas the Pb-containg ones are air stable. No obvious color changes are observed.

2) *Open tube preparations*: Equimolar amounts of MI_2 and AI were loaded in a 15mm pyrex test tubes. The materials were shaken mechanically to ensure a homogenous mixture. The tube was immersed in a sand bath standing at 350^{o}C under a gentle flow of nitrogen. The reaction proceeds within 0.5-1 min. The formation of a homogeneous black melt signals the end of the reaction. Upon melting the tube was removed from the bath and left to cool in air, usually producing a shiny black ingot. The melt is formed for the Sn-containing compounds only. Pb-containing solids decompose on prolonged heating (> 3 min) or by raising the temperature above 400^{o}C, through evolution of I_2 gas, crystallizing on the cooler walls of the tube. The shiny black ingots of the Sn-containing compounds are gradually converted into dull black/greenish solids within 24h.

3) *Room temperature solid state preparations*: Equimolar amounts of MI_2 and AI were placed in an agate mortar and ground carefully with a pestle until a visually homogeneous, black powder is obtained. The Sn-containing solids are air sensitive whereas the Pb-containg ones are air stable. No obvious color changes are observed.

Characterization

Thermal Analysis: The Thermogravimetric Analysis (TGA) measurements were performed on a Shimadzu TGA-50 thermogravimetric analyzer in aluminum boats under a N_2 flow. Differential Thermal Analysis (DTA) was performed on a Shimadzu DTA-50 thermal analyzer in aluminum boats using α-Al_2O_3 in identical aluminum boats as a reference, under a N_2 flow. Differential Scanning Calorimetry (DSC) measurements were performed on a DSC-60 calorimeter in aluminum boats using identical aluminum boats as a reference. The temperature range studied was 20-500 ^{o}C.

Scanning Electron Microscopy (SEM): Semiquantitative microprobe analyses and energy-dispersive spectroscopy (EDS) were performed with a Hitachi S-3400 scanning electron microscope equipped with a PGT energy-dispersive X-ray analyzer. Data were acquired with an accelerating voltage of 20 kV.

Powder X-ray diffraction studies: Powder X-ray diffraction measurements were performed using a silicon-calibrated CPS 120 INEL powder X-ray diffractometer (Cu Kα, 1.54056A°) graphite monochromatized radiation) operating at 40 kV and 20 mA, equipped with a position-sensitive detector with a flat sample geometry.

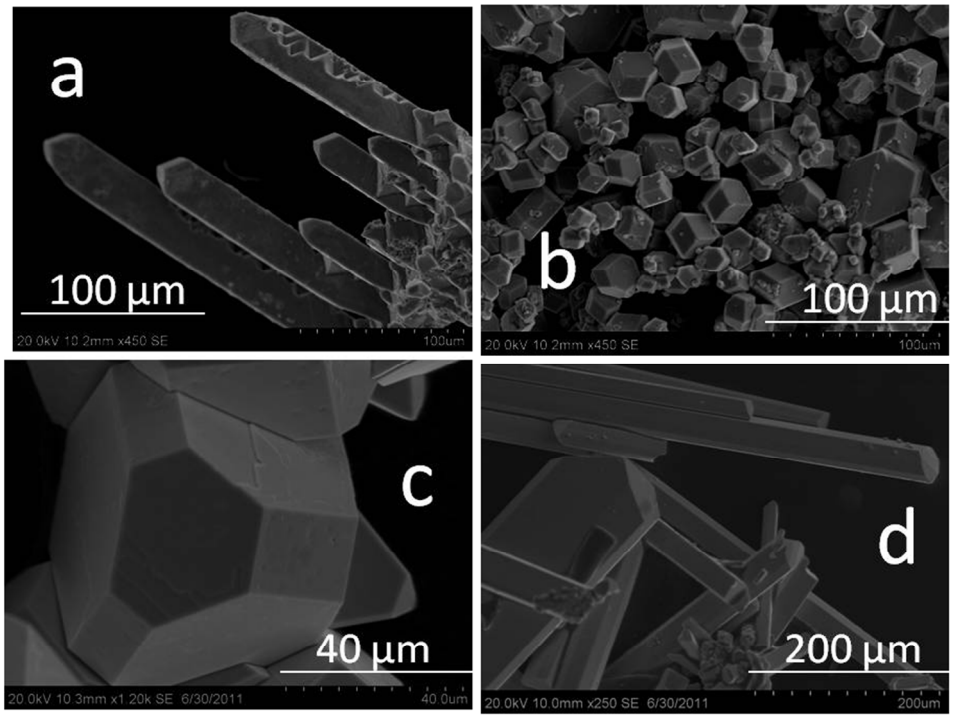

Figure S1. Crystals of (a) $CH_3NH_3SnI_3$ and (b) $HC(NH_2)_2SnI_3$ displaying elongated and normal rhombic dodecahedral symmetry. (c) Cs_2SnI_6 displays tetradecahedral crystallization habit forming truncated octahedra, the characteristic *fcc*-crystal habit. (d) $CsPbI_3$ forms large elongated needles, a typical crystal habit of the *P*nma space group.

X-ray diffraction measurements

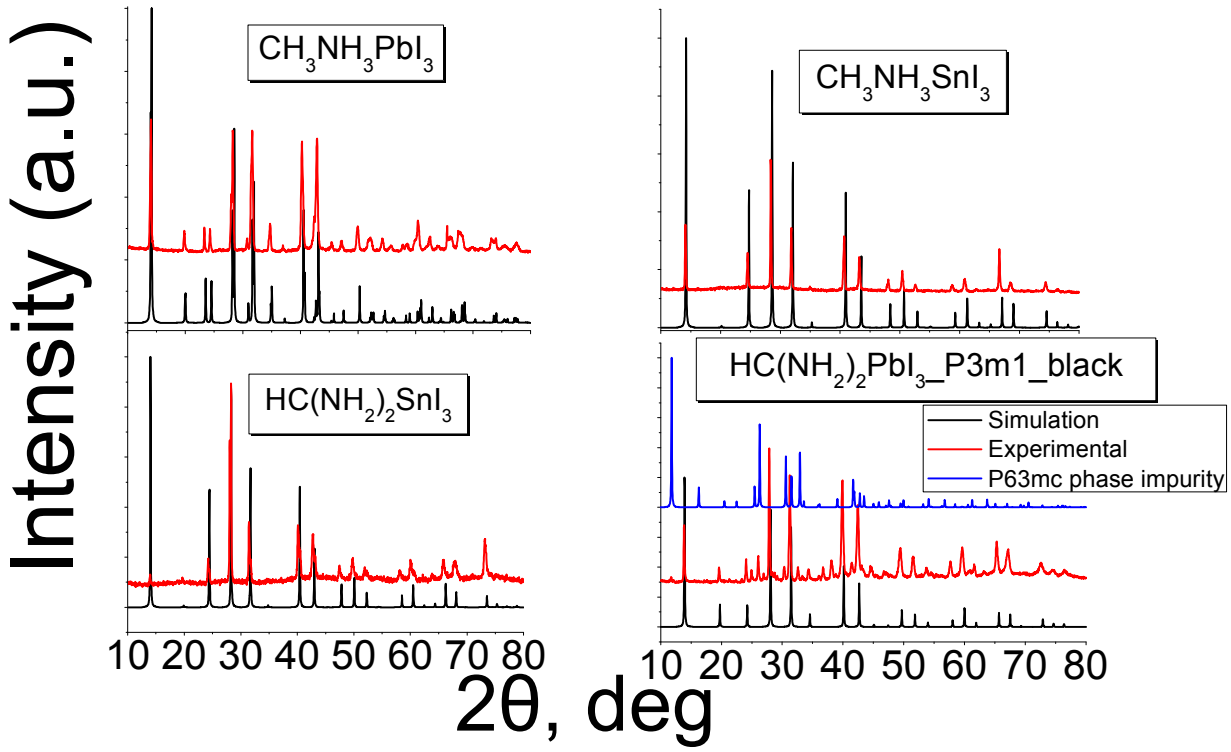

Figure S2. Experimental (red line) vs. Simulated (black line) powder patterns for compounds **1-4** prepared from solution. The pattern of $HC(NH_2)_2PbI_3$ requires both the simulated spectra of **4a** (black line) and **4b** (blue line) to account for all the experimentally observed peaks.

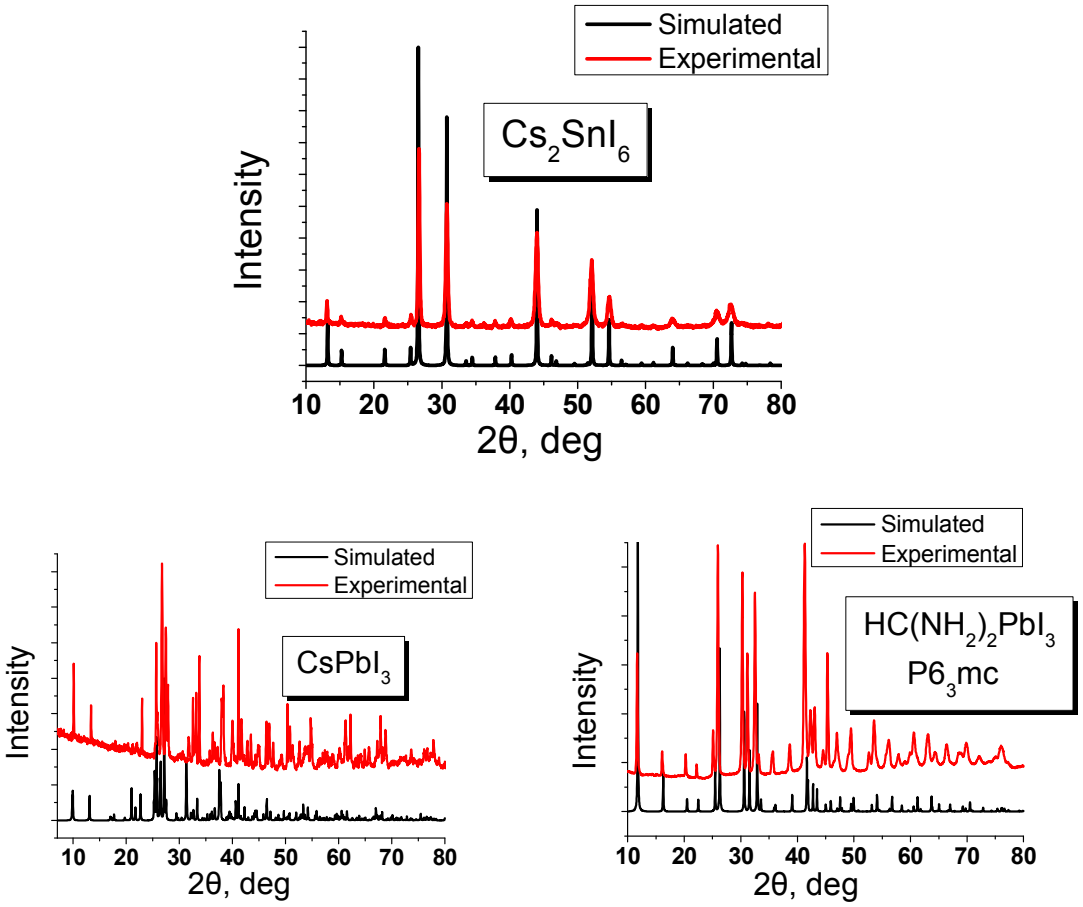

Figure S3. Experimental (black line) vs. Simulated (red line) powder patterns for compounds **7**, **6b** and **4b**, prepared from solution.

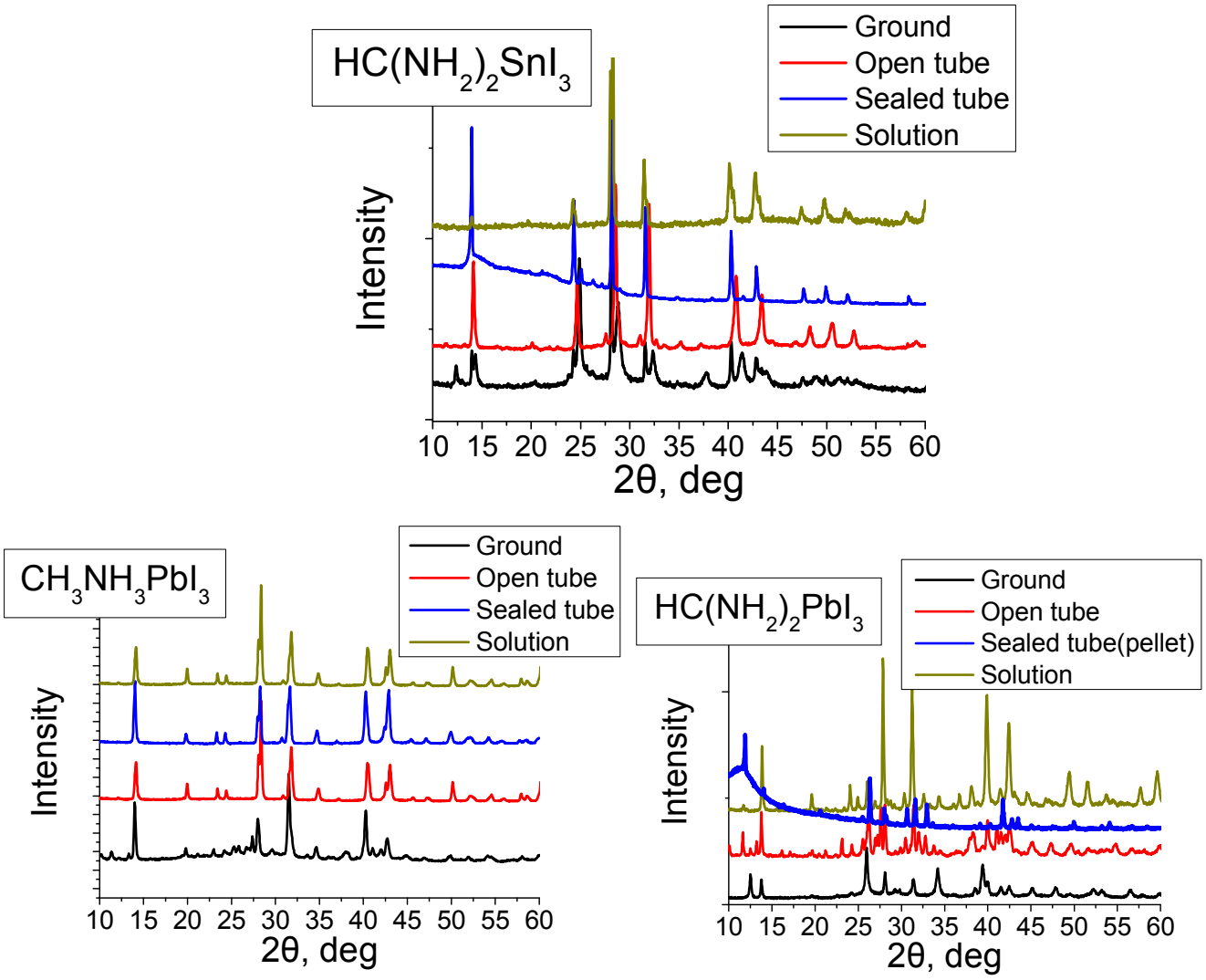

Figure S4. Powder diffraction patterns of **2-4** obtained by variation of the synthetic method.

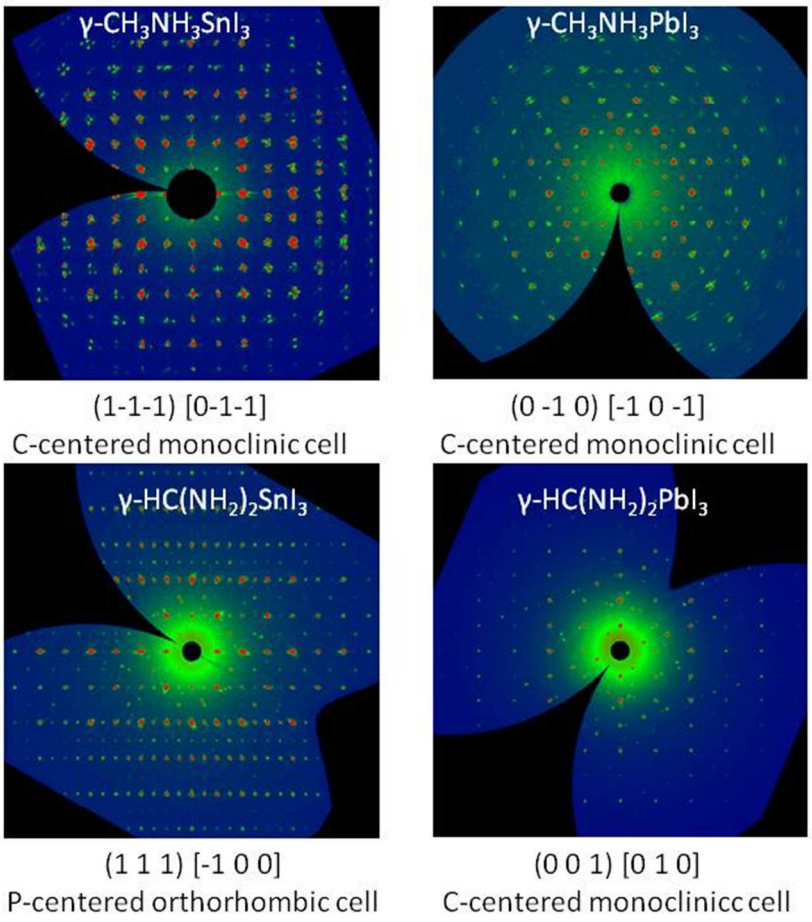

Figure S5. Precession images of single crystals for compounds **1**-**4** generated from data collected at 100K. The vectors used to generate the image at 000 point are noted underneath the respective figures, referring to the specific cell centering.

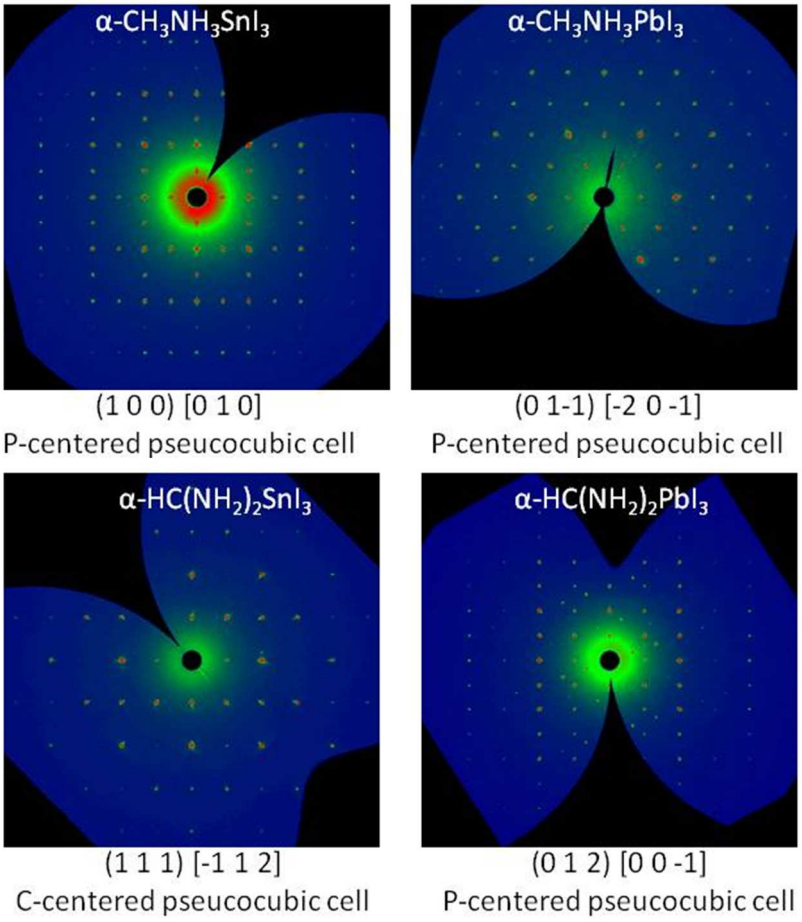

Figure S6. Precession images of single crystals for compounds **1**-**4** generated from data collected at 293K, except for α-$HC(NH_2)_2SnI_3$, which collected at 340K The vectors used to generate the image at 000 point are noted underneath the respective figures, referring to the specific cell centering.

Thermal analysis

Differential thermal analysis and differential scanning calorimetry studies were performed on the materials, aiming to detect any possible phase transitions that occur above room temperature. The only thermal event that could be detected between room temperature and the decomposition temperature was the evaporation of formamidine or a formamidine-related compound (endothermic) at 70^{o}C and an exothermic event for **4a** at 270^{o}C both of which are related to mass losses and are therefore irreversible.

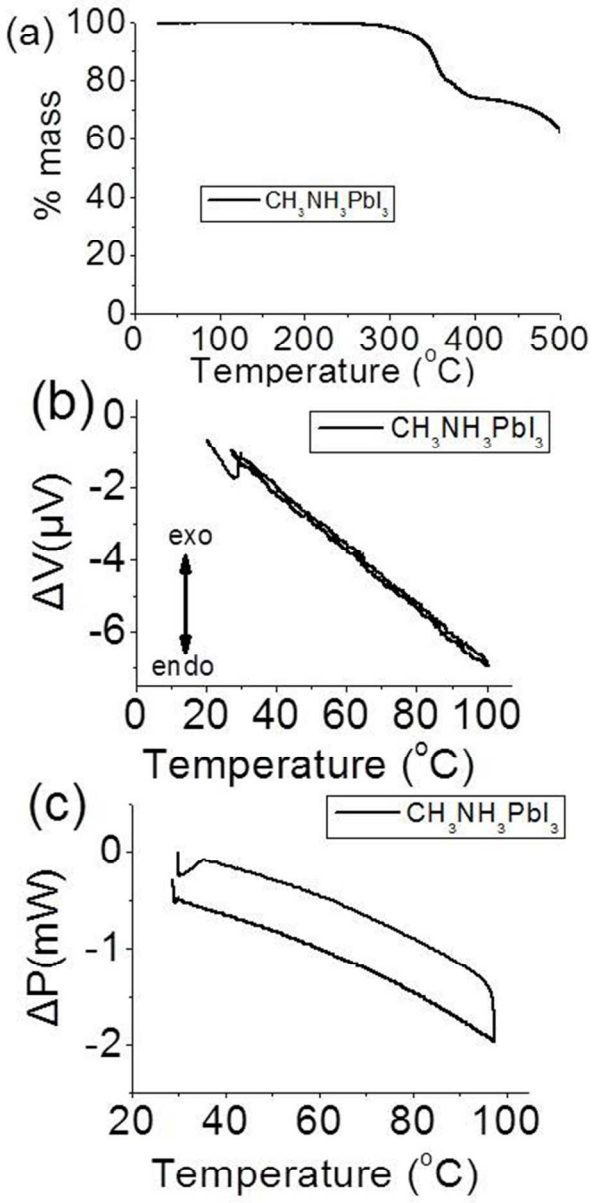

Figure S7. (a) TGA (5°C/min), (b) DTA (1°C/min) and (c) DSC (1°C/min) for $CH_3NH_3PbI_3$ prepared from the solution method. No obvious signals can be detected at the phase transition temperature range.

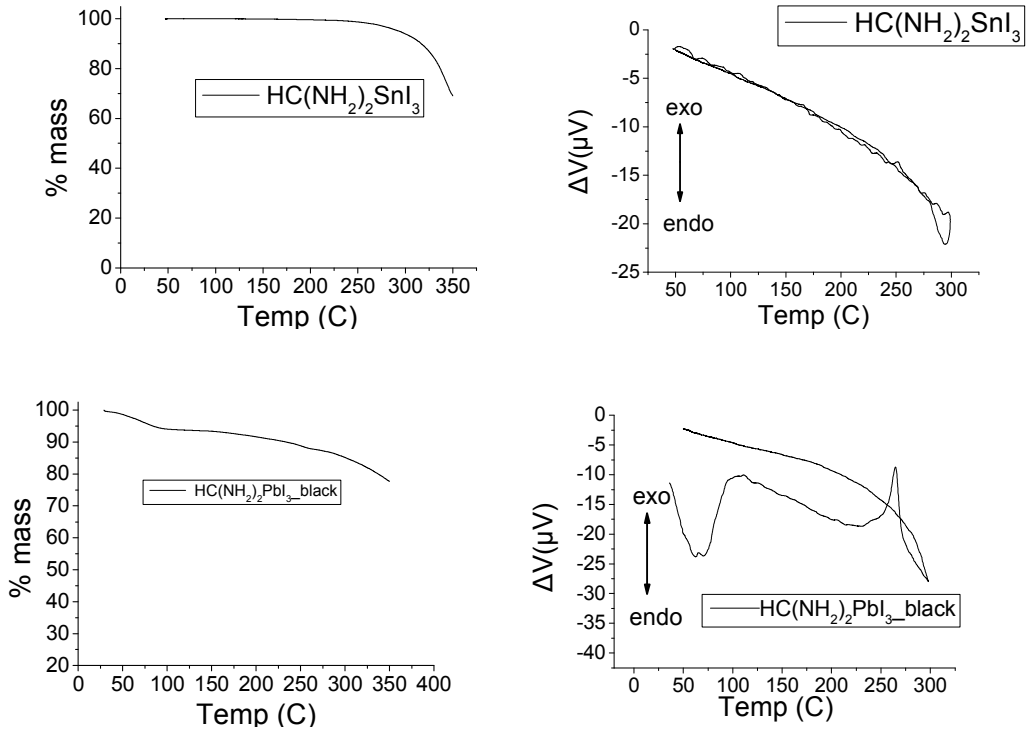

Figure S8. Thermal analysis plots for **2** (top) and **4a** (bottom)

PL measurements

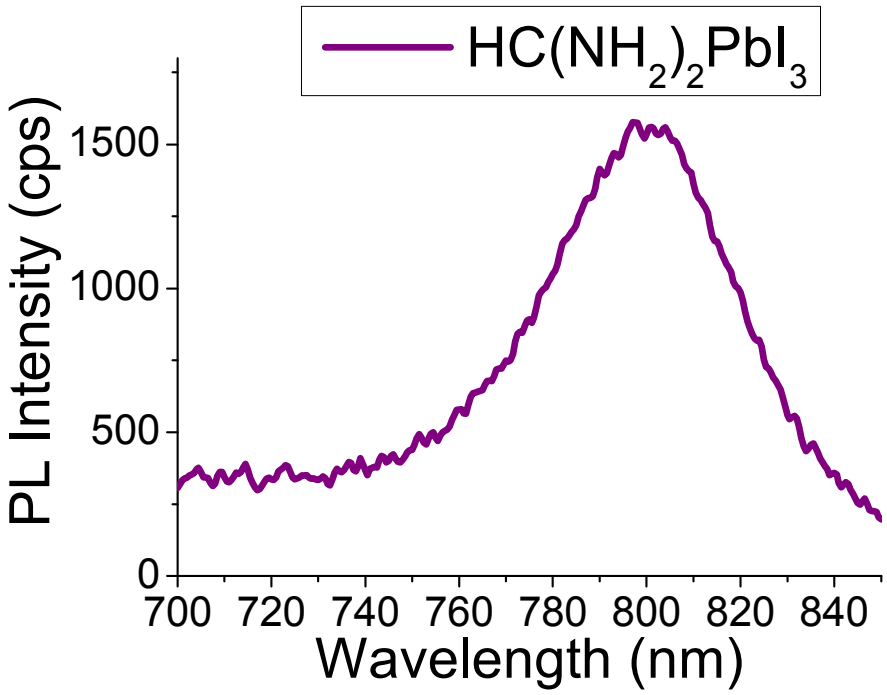

Figure S9. Photoluminescence properties of $HC(NH_2)_2PbI_3$ (**4**) from a sample obtained with the solution method.

Charge Transport measurements

Because of the non-ohmic, hysteretic behavior of $CH_3NH_3PbI_3$ it was difficult to estimate its true resistivity. The different values obtained from the PPMS and the conventional method are purely an issue of the measuring approach, with PPMS values obtained as an average of two measurements whereas in the conventional setup resistivity is calculated as a least-square fit of the experimental data. In fact, the values obtained from the two measurements converge into a single value when the resistivity of the conventional measurement method is plotted as an average of the "+" and "-" voltage polarity, which is the routine used in the PPMS setup. We suppose that the same or similar non-ohmic should apply for the β- and γ- phases of **1**, **2** and probably **4** and therefore the absolute values of resistivity are not reliable. They can only be accepted as they regard the trend of the experimental data.

The only reliable and consistently reproducible data come for the α-phases which displayed ohmic behavior (Figure S10).

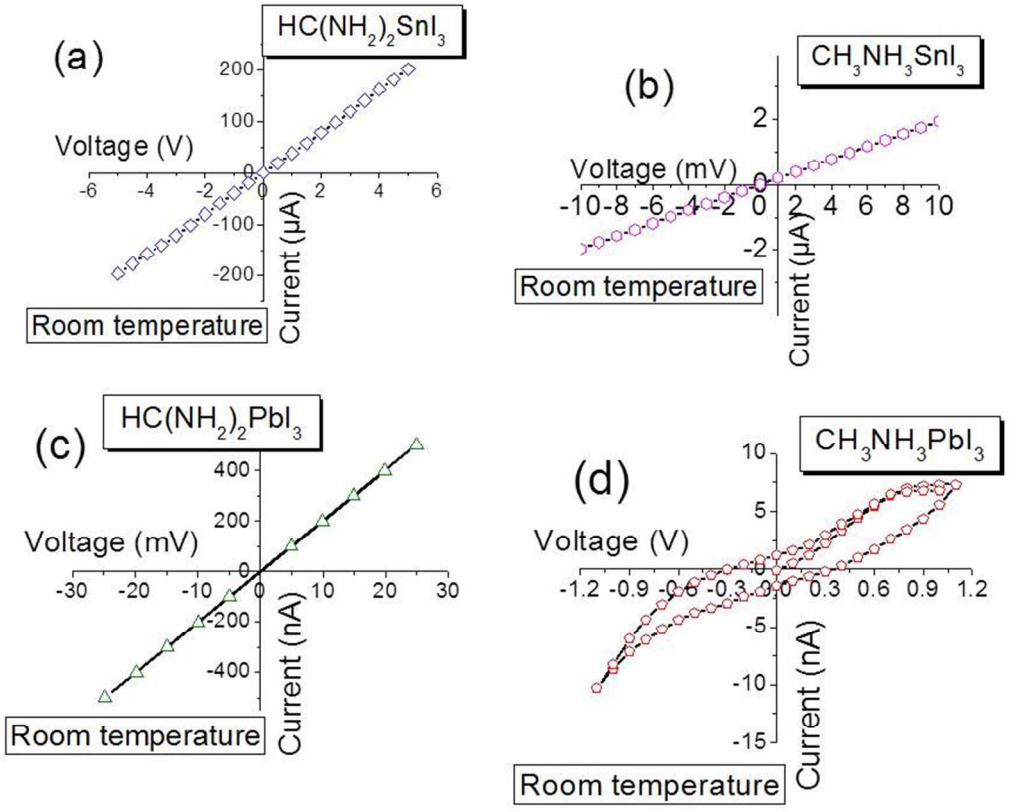

Figure S10. Room temperature I-V characteristics of single-crystals of **1**-**3** obtained from solution and an annealed pellet of **4a** obtained from the grinding method.

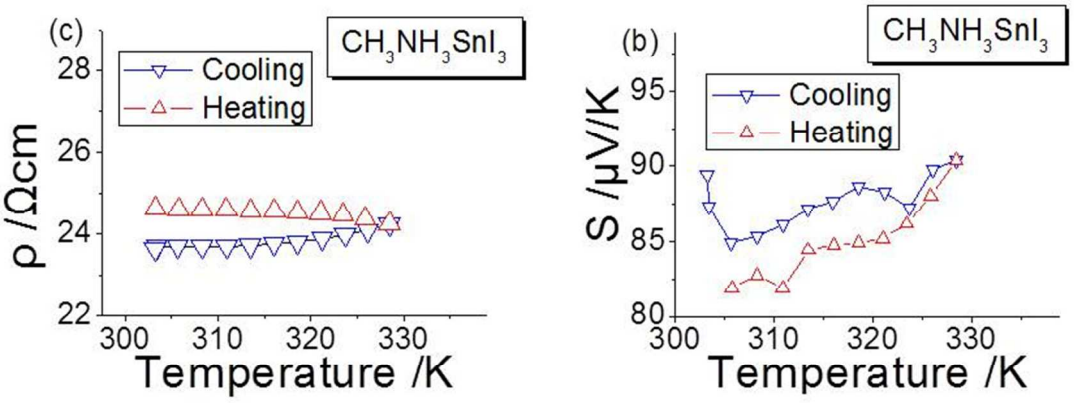

Figure S11. Resistivity and Seebeck coefficient plots of p-type $CH_3NH_3SnI_3$ prepared from the open tube method.

Mid-IR spectroscopy

The most pronounced indication of this difference between the Sn and Pb compounds comes from studying their mid-IR spectra. At this region, one should expect to observe only absorptions arising from the vibrational motion of the organic cations, which is in fact the case for compounds **3** and **4a** (Figure S12). However, in the case of Sn-based materials, these absorptions are masked by a broad absorption centered at ~1000 cm^{-1} (100 meV). This is possibly an intra-band transition close the top of the valence band between full $5s^2$ orbitals (Sn^{2+}) and (partially) vacant $5s^0$ orbitals (Sn^{4+}) based on band structure calculations on $ASnI_3$ compounds.[2] However, such a plasmon frequency requires a carrier concentration ~10^{18}-10^{19} cm^{-3} for a carrier effective mass of m_e=1 which is not supported by charge transport measurements. For $CH_3NH_3SnI_3$, where the largest and most intense plasmon frequency is observed a huge electron mobility is also observed, which suggests that the effective mass of the $CH_3NH_3SnI_3$ compound should be very small. A similar behavior also occurs for compound **2** though it is much less intense in magnitude, further supporting the mobility argument since $HC(NH_2)_2SnI_3$ has a significantly lower mobility than $CH_3NH_3SnI_3$.

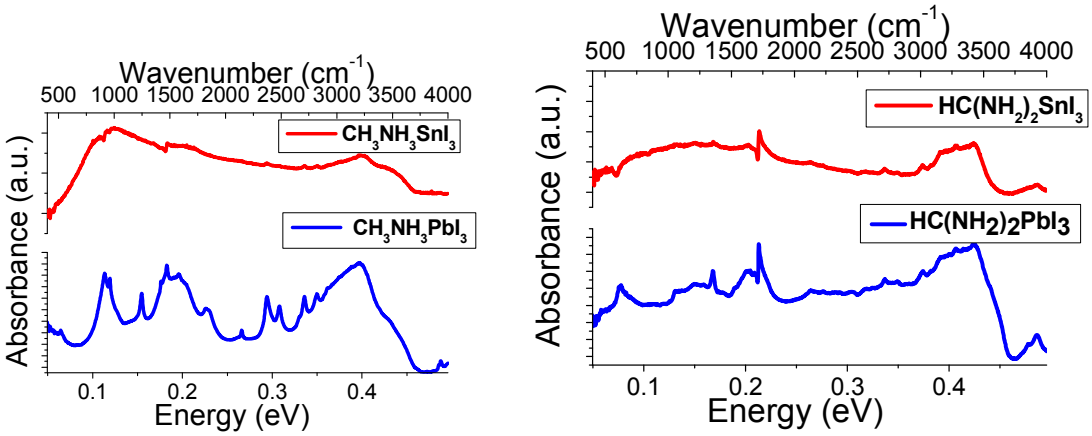

Figure S12. Mid-IR diffuse reflectance spectra for **1**-**4** prepared with the solution method.

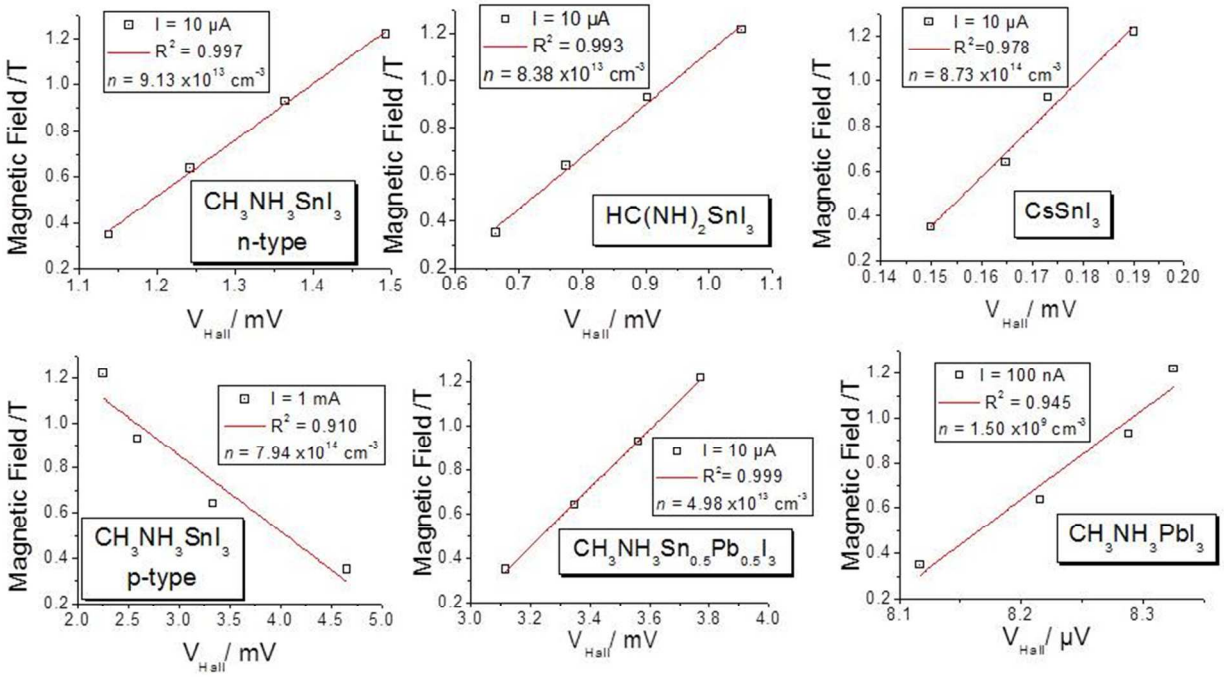

Figure S13. Hall effect plots of **1**-**3**, **5b** and $CsSnI_3$. All samples were prepared using the annealing method, except p-type $CH_3NH_3SnI_3$ which was prepared by the open tube method. Applied current and the calculated carrier concentration values are given in the respective panels.

Crystallographic Data

Table S1. Atomic coordinates ($x10^4$) and equivalent isotropic displacement parameters ($Å^2x10^3$) for **1** at 293(2) K with estimated standard deviations in parentheses.

Label	x	y	z	Occupancy	U_{eq}^*
Sn	0	0	9503	1	27(1)
I(1)	-5000	0	9615(13)	1	85(1)
I(2)	0	0	14629(7)	1	84(2)
C	5000	5000	3010(110)	1	170(40)
N	5000	5000	5170(110)	1	120(30)

*U_{eq} is defined as one third of the trace of the orthogonalized U_{ij} tensor.

Table S2. Anisotropic displacement parameters ($Å^2x10^3$) for **1** at 293(2) K with estimated standard deviations in parentheses.

Label	U_{11}	U_{22}	U_{33}	U_{12}	U_{13}	U_{23}
Sn	28(2)	28(2)	26(2)	0	0	0
I(1)	20(2)	119(2)	114(2)	0	0	0
I(2)	115(2)	115(2)	23(3)	0	0	0

The anisotropic displacement factor exponent takes the form: $-2\pi^2[h^2a^{*2}U_{11} + ... + 2hka^*b^*U_{12}]$.

Table S3. Atomic coordinates ($x10^4$) and equivalent isotropic displacement parameters ($Å^2x10^3$) for **1** at 200(2) K with estimated standard deviations in parentheses.

Label	x	y	z	Occupancy	U_{eq}^*
Sn	0	0	0(1)	1	23(1)
I(1)	0	0	2541(2)	1	41(1)
I(2)	2122(1)	7122(1)	59(2)	1	48(1)
N	5000	0	1743(12)	1	270(30)

C	5000	0	2854(12)	1	170(20)

*U_{eq} is defined as one third of the trace of the orthogonalized U_{ij} tensor.

Table S4. Anisotropic displacement parameters ($Å^2x10^3$) for **1** at 200(2) K with estimated standard deviations in parentheses.

Label	U_{11}	U_{22}	U_{33}	U_{12}	U_{13}	U_{23}
Sn	22(1)	22(1)	25(1)	0	0	0
I(1)	51(1)	51(1)	22(1)	0	0	0
I(2)	40(1)	40(1)	62(1)	22(1)	-16(1)	-16(1)

The anisotropic displacement factor exponent takes the form: $-2\pi^2[h^2a^{*2}U_{11} + ... + 2hka^*b^*U_{12}]$.

Table S5. Atomic coordinates ($x10^4$) and equivalent isotropic displacement parameters ($Å^2x10^3$) for **2** at 340(2) K with estimated standard deviations in parentheses.

Label	x	y	z	Occupancy	U_{eq}^*
Sn	5000	0	6186	1	51(1)
I(1)	5000	2494(3)	3753(3)	1	92(1)
I(2)	0	0	6243(7)	1	92(1)
N	1770(30)	0	1530(60)	1	285(18)
H(0A)	1855	0	2486	1	342
H(0B)	2900	0	994	1	342
C	0	0	910(80)	1	230(17)
H(0)	0	0	-133	1	276

*U_{eq} is defined as one third of the trace of the orthogonalized U_{ij} tensor.

Table S6. Anisotropic displacement parameters ($Å^2x10^3$) for **2** at 340(2) K with estimated standard deviations in parentheses.

Label	U_{11}	U_{22}	U_{33}	U_{12}	U_{13}	U_{23}
Sn	50(1)	53(1)	51(1)	0	0	0
I(1)	111(1)	84(1)	82(1)	0	0	36(1)
I(2)	45(1)	117(1)	113(2)	0	0	0

The anisotropic displacement factor exponent takes the form: $-2\pi^2[h^2a^{*2}U_{11} + ... + 2hka^*b^*U_{12}]$.

Table S7. Atomic coordinates ($x10^4$) and equivalent isotropic displacement parameters ($Å^2x10^3$) for **2** at 180(2) K with estimated standard deviations in parentheses.

Label	x	y	z	Occupancy	U_{eq}^*
Sn	2500(1)	2498(1)	3261(1)	1	28(1)
I(1)	2549(1)	2496(1)	717(1)	1	46(1)
I(2)	0	2225(1)	8237(1)	1	57(1)
I(3)	0	2244(1)	3126(1)	1	59(1)
I(4)	2708(1)	0	3224(2)	1	60(1)
I(5)	2821(1)	0	8227(1)	1	46(1)
C(3)	0	0	0	1	24
N(2)	0	4080	5909	1	70
N(1)	0	4040	849	1	53
C(2)	0	5000	6498	1	53

C(1)	0	5000	374	1	30
N(4)	976	0	787	1	44
C(4)	0	0	6069	1	48
N(3)	955	0	5386	1	75

*U_{eq} is defined as one third of the trace of the orthogonalized U_{ij} tensor.

Table S8. Anisotropic displacement parameters ($Å^2x10^3$) for **2** at 180(2) K with estimated standard deviations in parentheses.

Label	U_{11}	U_{22}	U_{33}	U_{12}	U_{13}	U_{23}
Sn	30(1)	29(1)	26(1)	0(1)	0(1)	-1(1)
I(1)	58(1)	56(1)	25(1)	0(1)	-2(1)	8(1)
I(2)	27(1)	79(1)	64(1)	0	0	5(1)
I(3)	23(1)	80(1)	74(1)	0	0	-37(1)
I(4)	93(1)	31(1)	55(1)	0	-6(1)	0
I(5)	59(1)	20(1)	59(1)	0	-14(1)	0

The anisotropic displacement factor exponent takes the form: $-2\pi^2[h^2a^{*2}U_{11} + ... + 2hka^*b^*U_{12}]$.

Table S9. Atomic coordinates ($x10^4$) and equivalent isotropic displacement parameters ($Å^2x10^3$) for **3** at 400(2) K with estimated standard deviations in parentheses.

Label	x	y	z	Occupancy	U_{eq}^*
Pb	5000	5000	5081(2)	1	46(1)
I(1)	5000	0	5122(17)	1	132(1)
I(2)	5000	5000	-6(5)	1	132(2)
C	0	0	-1010(50)	1	116(18)
N	0	0	1180(70)	1	300(90)

*U_{eq} is defined as one third of the trace of the orthogonalized U_{ij} tensor.

Table S10. Anisotropic displacement parameters ($Å^2x10^3$) for **3** at 400(2) K with estimated standard deviations in parentheses.

Label	U_{11}	U_{22}	U_{33}	U_{12}	U_{13}	U_{23}
Pb	47(1)	47(1)	46(1)	0	0	0
I(1)	181(2)	36(1)	178(2)	0	0	0
I(2)	181(2)	181(2)	32(1)	0	0	0

The anisotropic displacement factor exponent takes the form: $-2\pi^2[h^2a^{*2}U_{11} + ... + 2hka^*b^*U_{12}]$.

Table S11. Atomic coordinates ($x10^4$) and equivalent isotropic displacement parameters ($Å^2x10^3$) for **3** at 293(2) K with estimated standard deviations in parentheses.

Label	x	y	z	Occupancy	U_{eq}^*
Pb	0	0	0	1	32(1)
I(1)	0	0	2472(7)	1	79(1)
I(2)	2142(2)	7142(2)	46(6)	1	83(1)
C	5000	0	3520(110)	1	340(100)
N	5000	0	2420(110)	1	170(20)

$^*U_{eq}$ is defined as one third of the trace of the orthogonalized U_{ij} tensor.

Table S12. Anisotropic displacement parameters ($Å^2x10^3$) for **3** at 293(2) K with estimated standard deviations in parentheses.

Label	U_{11}	U_{22}	U_{33}	U_{12}	U_{13}	U_{23}
Pb	32(1)	32(1)	32(1)	0	0	0
I(1)	107(1)	107(1)	24(2)	0	0	0
I(2)	68(1)	68(1)	113(2)	43(1)	28(2)	28(2)

The anisotropic displacement factor exponent takes the form: $-2\pi^2[h^2a^{*2}U_{11} + ... + 2hka^*b^*U_{12}]$.

Table S13. Atomic coordinates ($x10^4$) and equivalent isotropic displacement parameters ($Å^2x10^3$) for **4a** at 293(2) K with estimated standard deviations in parentheses.

Label	x	y	z	Occupancy	U_{eq}*
Pb(1)	6667	3333	8379(1)	1	49(1)
Pb(2)	0	0	5045(1)	1	49(1)
Pb(3)	3333	6667	1709(2)	1	26(1)
I(1)	1662(1)	8338(1)	3376(1)	1	93(1)
I(2)	8330(2)	1670(2)	6711(2)	1	93(1)
I(3)	4996(1)	5004(1)	45(1)	1	94(1)
C(2)	3333	6667	6138(1)	1	250(20)
N(2)	4015(8)	5985(8)	6138(1)	0.67	123(5)
C(1)	6667	3333	3426(1)	1	83(4)
N(1)	5903(9)	4097(9)	3426(1)	0.67	340(20)
C(3)	0	0	107(1)	1	255(18)
N(3)	771(9)	1543(19)	107(1)	0.67	410(30)

*U_{eq} is defined as one third of the trace of the orthogonalized U_{ij} tensor.

Table S14. Anisotropic displacement parameters ($Å^2x10^3$) for **4a** at 293(2) K with estimated standard deviations in parentheses.

Label	U_{11}	U_{22}	U_{33}	U_{12}	U_{13}	U_{23}
Pb(1)	50(1)	50(1)	46(1)	25(1)	0	0
Pb(2)	48(1)	48(1)	50(1)	24(1)	0	0
Pb(3)	26(1)	26(1)	26(1)	13(1)	0	0
I(1)	108(1)	108(1)	94(1)	76(1)	22(1)	-22(1)
I(2)	107(1)	107(1)	94(1)	76(1)	21(1)	-21(1)
I(3)	111(1)	111(1)	92(1)	78(1)	21(1)	-21(1)

The anisotropic displacement factor exponent takes the form: $-2\pi^2[h^2a^{*2}U_{11} + ... + 2hka^*b^*U_{12}]$.

Table S15. Atomic coordinates ($x10^4$) and equivalent isotropic displacement parameters ($Å^2x10^3$) for **4a** at 150(2) K with estimated standard deviations in parentheses.

Label	x	y	z	Occupancy	U_{eq}^*
Pb(1)	3332(1)	1665(1)	1994(1)	1	38(1)
Pb(2)	5000(1)	0(1)	5327(1)	1	26(1)
Pb(3)	1668(1)	3335(1)	8664(1)	1	31(1)
Pb(4)	3333	6667	1995(2)	1	36(1)
Pb(5)	6667	3333	8657(2)	1	44(1)
Pb(6)	0	0	5330(1)	1	16(1)
I(1)	4209(2)	3442(1)	3439(2)	1	91(1)
I(2)	2555(1)	2450(1)	104(2)	1	92(1)
I(3)	3230(1)	4094(1)	6768(2)	1	92(1)
I(4)	1654(1)	1002(1)	3667(2)	1	102(1)
I(5)	2684(1)	5024(1)	332(2)	1	101(1)
I(6)	6009(1)	1675(1)	7000(2)	1	102(1)
I(7)	798(1)	4227(1)	7188(2)	1	93(1)
I(8)	101(1)	2536(1)	510(2)	1	89(1)
I(9)	4138(1)	900(1)	3852(2)	1	92(1)
I(10)	4984(1)	2359(1)	340(2)	1	81(1)
I(11)	1656(1)	5690(1)	3676(2)	1	80(1)
I(12)	700(1)	1678(1)	6990(2)	1	79(1)
C(1)	380(5)	4676(6)	815(9)	1	36(2)
N(1)	5024(3)	112(6)	271(4)	1	36(2)
N(2)	637(2)	4429(2)	1745(4)	1	36(2)

C(2)	3268(5)	1592(5)	6939(10)	1	25(2)
N(3)	3070(2)	2005(2)	6186(4)	1	25(2)
N(4)	3660(2)	1290(2)	7542(5)	1	25(2)
C(3)	1344(11)	3364(7)	4463(16)	1	109(4)
N(5)	2093(5)	4109(3)	4464(9)	1	109(4)
N(6)	930(6)	2640(3)	3804(9)	1	109(4)
C(4)	0	0	90(50)	1	149(12)
N(7)	933(2)	500(18)	9890(40)	0.67	149(12)
C(5)	3333	6667	7520(40)	1	166(15)
N(8)	2468(1)	6535(2)	7838(8)	0.67	166(15)
C(6)	6667	3333	3260(40)	1	124(10)
N(9)	6287(9)	2404(2)	3050(30)	0.67	124(10)

*U_{eq} is defined as one third of the trace of the orthogonalized U_{ij} tensor.

Table S16. Anisotropic displacement parameters ($Å^2x10^3$) for **4a** at 150(2) K with estimated standard deviations in parentheses.

Label	U_{11}	U_{22}	U_{33}	U_{12}	U_{13}	U_{23}
Pb(1)	31(1)	41(1)	52(1)	27(1)	-4(1)	5(1)
Pb(2)	25(1)	32(1)	24(1)	17(1)	-8(1)	-16(1)
Pb(3)	51(1)	29(1)	21(1)	25(1)	0(1)	12(1)
Pb(4)	45(1)	45(1)	16(1)	23(1)	0	0
Pb(5)	46(1)	46(1)	38(1)	23(1)	0	0
Pb(6)	8(1)	8(1)	34(1)	4(1)	0	0
I(1)	154(1)	54(1)	59(1)	48(1)	-9(1)	-32(1)
I(2)	112(1)	149(1)	59(1)	98(1)	-17(1)	9(1)
I(3)	54(1)	122(2)	55(1)	11(1)	35(1)	26(1)
I(4)	102(1)	100(1)	109(1)	54(1)	77(1)	41(1)
I(5)	94(1)	99(1)	103(1)	43(1)	-42(1)	-90(1)
I(6)	90(1)	109(1)	105(1)	49(1)	-34(1)	-80(1)
I(7)	170(1)	121(1)	60(1)	126(1)	5(1)	17(1)
I(8)	30(1)	156(2)	54(1)	25(1)	17(1)	4(1)
I(9)	158(1)	123(1)	59(1)	117(1)	6(1)	14(1)
I(10)	50(1)	53(1)	139(1)	25(1)	54(1)	19(1)
I(11)	54(1)	57(1)	128(1)	27(1)	54(1)	24(1)
I(12)	55(1)	50(1)	133(1)	26(1)	-30(1)	-58(1)

The anisotropic displacement factor exponent takes the form: $-2\pi^2[h^2a^{*2}U_{11} + ... + 2hka^*b^*U_{12}]$.

Table S17. Atomic coordinates ($x10^4$) and equivalent isotropic displacement parameters ($Å^2x10^3$) for **4b** at 293(2) K with estimated standard deviations in parentheses.

Label	x	y	z	Occupancy	U_{eq}^*
Pb	0	0	60(70)	1	52(1)
I	8312(1)	1688(1)	2510(70)	1	73(1)
N	4090(30)	5910(30)	1549(2)	0.67	350(90)
C	3333	6667	1549(2)	1	99(17)

$^*U_{eq}$ is defined as one third of the trace of the orthogonalized U_{ij} tensor.

Table S18. Anisotropic displacement parameters ($Å^2x10^3$) for **4b** at 293(2) K with estimated standard deviations in parentheses.

Label	U_{11}	U_{22}	U_{33}	U_{12}	U_{13}	U_{23}
Pb	52(1)	52(1)	52(1)	26(1)	0	0
I	84(1)	84(1)	80(1)	64(1)	3(2)	-3(2)

The anisotropic displacement factor exponent takes the form: $-2\pi^2[h^2a^{*2}U_{11} + ... + 2hka^*b^*U_{12}]$.

Table S19. Atomic coordinates ($x10^4$) and equivalent isotropic displacement parameters ($Å^2x10^3$) for **5b** at 293(2) K with estimated standard deviations in parentheses.

Label	x	y	z	Occupancy	U_{eq}^*
Pb	0	0	2	0.569(7)	42(1)
Sn	0	0	2	0.431(7)	42(1)
I(1)	2269(2)	7269(2)	-7(5)	1	102(1)
I(2)	0	0	2548(4)	1	131(2)
C	5000	0	2227(19)	1	51(12)
N	5000	0	3320(30)	1	280(100)

*U_{eq} is defined as one third of the trace of the orthogonalized U_{ij} tensor.

Table S20. Anisotropic displacement parameters ($Å^2x10^3$) for **5b** at 293(2) K with estimated standard deviations in parentheses.

Label	U_{11}	U_{22}	U_{33}	U_{12}	U_{13}	U_{23}
Pb	38(1)	38(1)	50(1)	0	0	0
Sn	38(1)	38(1)	50(1)	0	0	0
I(1)	84(1)	84(1)	137(2)	48(1)	-41(2)	-41(2)
I(2)	179(3)	179(3)	36(2)	0	0	0

The anisotropic displacement factor exponent takes the form: $-2\pi^2[h^2a^{*2}U_{11} + ... + 2hka^*b^*U_{12}]$.

Table S21. Atomic coordinates ($x10^4$) and equivalent isotropic displacement parameters ($Å^2x10^3$) for **6b** at 293(2) K with estimated standard deviations in parentheses.

Label	x	y	z	Occupancy	U_{eq}^*
I	2454(1)	0	0	1	36(1)
Cs	2500	2500	2500	1	43(1)
Sn	0	0	0	1	21(1)

*U_{eq} is defined as one third of the trace of the orthogonalized U_{ij} tensor.

Table S22. Anisotropic displacement parameters ($Å^2x10^3$) for **6b** at 293(2) K with estimated standard deviations in parentheses.

Label	U_{11}	U_{22}	U_{33}	U_{12}	U_{13}	U_{23}
I	22(1)	44(1)	44(1)	0	0	0
Cs	43(1)	43(1)	43(1)	0	0	0
Sn	21(1)	21(1)	21(1)	0	0	0

The anisotropic displacement factor exponent takes the form: $-2\pi^2[h^2a^{*2}U_{11} + ... + 2hka^*b^*U_{12}]$.

Table S23. Atomic coordinates ($x10^4$) and equivalent isotropic displacement parameters ($Å^2x10^3$) for **7** at 293(2) K with estimated standard deviations in parentheses.

Label	x	y	z	Occupancy	U_{eq}^*
Pb	1604(1)	2500	4380(1)	1	28(1)
I(1)	1632(1)	2500	16(1)	1	32(1)
I(2)	2991(1)	2500	2873(1)	1	33(1)
I(3)	319(1)	2500	6145(1)	1	30(1)
Cs	4156(1)	2500	6709(1)	1	35(1)

*U_{eq} is defined as one third of the trace of the orthogonalized U_{ij} tensor.

Table S24. Anisotropic displacement parameters ($Å^2x10^3$) for **7** at 293(2) K with estimated standard deviations in parentheses.

Label	U_{11}	U_{22}	U_{33}	U_{12}	U_{13}	U_{23}
Pb	30(1)	27(1)	26(1)	0	2(1)	0
I(1)	31(1)	29(1)	35(1)	0	6(1)	0
I(2)	33(1)	37(1)	28(1)	0	4(1)	0
I(3)	26(1)	36(1)	26(1)	0	-2(1)	0
Cs	37(1)	35(1)	34(1)	0	0(1)	0

The anisotropic displacement factor exponent takes the form: $-2\pi^2[h^2a^{*2}U_{11} + ... + 2hka^*b^*U_{12}]$.

Table S25. The lattice parameters (Cu Kα) of the $CH_3NH_3Sn_{1-x}Pb_xI_3$ solid solution as calculated for the solids prepared through the annealing method and compared with the simulated data (Cu Kα).

Comp.	**SGR**	**a (Å)**	**b (Å)**	**c (Å)**	**α=β=γ (°)**	**Volume ($Å^3$)**
$CH_3NH_3SnI_3$_simul	*P*4mm	6.230 (1)	6.230(1)	6.231(1)	90	241.88(7)
$CH_3NH_3SnI_3$	*P*4mm	6.245(1)	6.245(1)	6.249(4)	90	243.71(12)
$CH_3NH_3Sn_{0.75}Pb_{0.25}I_3$	*P*4mm	6.281(1)	6.281(1)	6.300(3)	90	248.53(13)
$CH_3NH_3Sn_{0.50}Pb_{0.50}I_3$	*I*4cm	8.918(1)	8.918(1)	12.714(8)	90	1011.04(60)
$CH_3NH_3Sn_{0.46}Pb_{0.54}I_3$_simul	*I*4cm	8.855(1)	8.855(1)	12.535(1)	90	982.95(13)
$CH_3NH_3Sn_{0.25}Pb_{0.75}I_3$	*I*4cm	8.946(1)	8.946(1)	12.728(8)	90	1018.68(61)
$CH_3NH_3PbI_3$	*I*4cm	8.979(1)	8.979(1)	12.590(8)	90	1015.06(59)
$CH_3NH_3PbI_3$_simul	*I*4cm	8.8494(13)	8.8494(13)	12.642(3)	90	990.02(4)

References

(1) Howie, R. A.; Moser, W.; Trevena, I. C. *Acta Crystallogr. Sect. B* **1972**, *28*, 2965.

(2) Borriello, I.; Cantele, G.; Ninno, D. *Phys. Rev. B* **2008**, *77*, 235214.